Fusion Engineering and Design 123 (2017) 435–439

Contents lists available at ScienceDirect

Fusion Engineering and Design

journal homepage: www.elsevier.com/locate/fusengdes

Electron cyclotron stray radiation detection and machine protection system proposal for JT-60SA

A. Moro[a,*], S. Coda[b], D. Douai[c], D. Farina[a], L. Figini[a], T. Goodman[b], A. Isayama[d], T. Kobayashi[d], D. Micheletti[a], S. Moriyama[d], P. Platania[a], D. Ricci[a], C. Sozzi[a]

[a] Istituto di Fisica del Plasma "Piero Caldirola" CNR, Milano, Italy
[b] Swiss Plasma Center, EPFL, CH-1015 Lausanne, Switzerland
[c] CEA, IRFM, F-13108 Saint-Paul-Lez-Durance, France
[d] National Institutes for Quantum and Radiological Science and Technology QST, Naka, Ibaraki 311-0193, Japan

HIGHLIGHTS

- Analysis on EC operations characterized by low absorption and therefore high levels of stray radiation in JT-60SA.
- Qualitative and quantitative evaluation of the expected wall loads and diffuse EC stray radiation amount.
- Proposal for a protection system relying on pyrodetectors and examples of a similar system installed on TCV tokamak, used during wall cleaning experiments with EC waves.

ARTICLE INFO

Article history:
Received 2 October 2016
Received in revised form 11 February 2017
Accepted 7 March 2017
Available online 3 April 2017

Keywords:
Electron cyclotron
Stray radiation
Machine protection

ABSTRACT

The JT-60SA tokamak is scheduled to start operations in 2019 to support the ITER experimental programme and to provide key information for the design of DEMO scenarios. The device will count on ECRH and NBI as auxiliary heating. Potentially dangerous situations that could harm the tokamak structures during operations characterized by low EC absorption cannot be a priori excluded. An estimation of the wall load under direct beam exposure and during plasma operations will be given, using the EC antenna main characteristics and launching geometry. A system capable to prevent the risk of damage to machine components for JT-60SA is presented and examples of potential benefits of such a system will be given, based on recent experience gained on the TCV tokamak during EC wall cleaning experiments performed in preparation of JT-60SA operations.

1. Introduction

JT-60SA is a fully superconducting tokamak device being built under the Broader Approach Satellite Tokamak Programme jointly by Europe and Japan. The start of operations is planned for 2019 [1] and the machine will be one of the main actors the fusion programme supporting the ITER experimental programme as a satellite device and providing guidelines for the design of DEMO reactor scenarios. ECRH operations are foreseen in various applications: Electron Cyclotron (EC) assisted startup, EC wall conditioning, bulk heating and current drive and magneto-hydrodynamic instabilities control to cite some with 7 MW of total injected EC power, at three different operating frequencies: 82 GHz, 110 GHz and 138 GHz. The use of the ECRH system, in particular for plasma initiation, requires a careful analysis of the EC stray radiation, both with modelling in the various conditions of low absorption and with studies of the possible detection systems. Such studies are here presented in this paper with qualitative and quantitative evaluation of the expected wall loads and diffuse EC stray radiation amount, with the aim to provide a proposal for a protection system relying on appropriate detectors. To reach this, examples of a similar system installed on TCV tokamak and used during wall cleaning experiments with EC waves will also be given.

2. ECRH system in JT-60SA and low absorption scenarios

The ECRH system for JT-60SA will consist of 9 gyrotrons (1 MW each) enabling dual frequency operations at 110 GHz and 138 GHz

* Corresponding author.
E-mail address: moro@ifp.cnr.it (A. Moro).

http://dx.doi.org/10.1016/j.fusengdes.2017.03.028

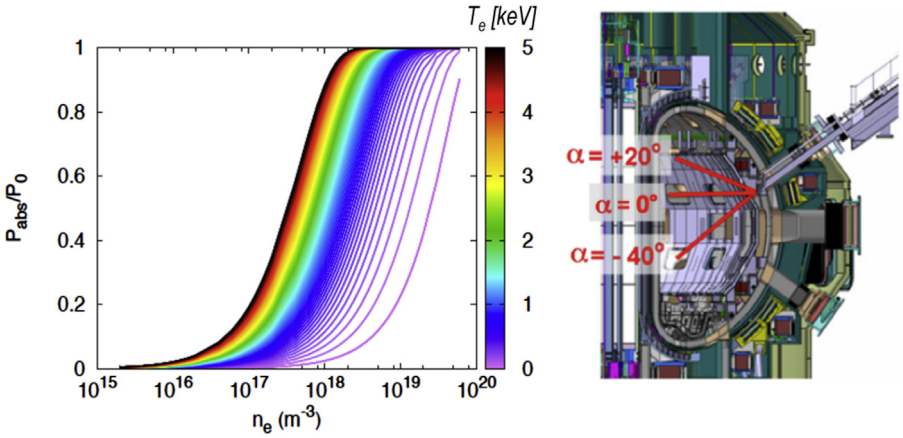

Fig. 1. Left: EC absorbed power fraction versus density for various temperature. Right: model of the poloidal cross-section of JT-60SA showing one of the ECRF launchers and extreme poloidal injection angles available in terms of poloidal angle α.

for second harmonic extraordinary mode (XM2) absorption and providing 7 MW injection for 100 s pulse length [2]. Four launchers will be installed and used for local heating, current drive and plasma initiation by injection of high-power and long-pulse waves into the plasma. The initial research phase will rely on 4 gyrotrons and the additional frequency of 82 GHz for short pulses (<1 s) is being developed for the same gyrotron [3], candidate for wall cleaning and EC assisted startup experiments. Except for the initial phase (up to 3 MW of ECRH available) the nominal total EC power available will be 7 MW [5]. The dedicated Ports for EC waves injection are upper outboard ports P-01, P-04, P-08, P-11. The requirements of a wide poloidal injection angle range has driven a front steering antenna design with a first mirror with linear and rotation motions and a fixed second mirror [4].

Critical phases characterized by low absorption and therefore high levels of EC stray radiation that could harm tokamak structures will be assisted breakdown, EC wall cleaning and all those operating mode where not optimal EC absorption could be present, which include high density scenarios. Not absorbed power will be reflected from the stabilizing plate and/or vessel wall, and after some bounces diffuse radiation will fill the vessel and reach outer regions and vacuum windows via chamber openings. In the case of plasma breakdown EC power will be injected in JT-60SA chamber at the beginning of discharge in order to assist gas ionization and plasma formation (breakdown). In this phase RF power absorption from the plasma may be low, due to low temperature and density conditions prior to ionization and breakdown. Different configurations can be considered regarding operating modes, defined by the magnetic field of a given scenario and by the EC wave frequency, which could consist of ordinary mode (OM) or extraordinary mode (XM) in fundamental or higher harmonics. In the case of XM2 assisted breakdown, a low toroidal angle must be considered to maintain good second pass absorption. XM2 has in fact a good first pass absorption but after the reflection is converted in OM2 (being mode conversion more efficient for large toroidal injection angles) that has a negligible absorption. In order to simulate and optimise the electron cyclotron assisted break-down and plasma start-up in JT-60SA, the 0D plasma transport model BKD0 has been developed [6]. It simulates the evolution of the plasma parameters considering the energy balance equations for electrons and ions, the particle balance equation for electrons, ions and neutrals and the circuit equation. The EC power absorption has been estimated self-consistently coupling BKD0 with the quasi-optical beam tracing code GRAY [7]. Injection of 110 GHz EC (XM2) has been investigated for two different poloidal injection angles ($\alpha = -19^\circ$ and $\alpha = -27^\circ$, aiming the EC power deposition in the null region).[1] Evaluations from 0-D code BKD0 coupled to EC beam tracing code GRAY give indications on possible waves absorption during start-up phase, as shown in Fig. 1, where parameters from Scenario 5 ($f = 110$ GHz $B = 1.7$ T) and magnetic field map in early time slice have been used to compute expected EC absorption as a function of plasma density (Fig. 1 left) and limit prefill pressure as a function of injected EC power (Fig. 1 right). It can be seen that for temperatures in the range [50–150] eV and electron density 2×10^{18} m^{-3} (these values can be considered as reference values at early discharge stage, with startup to be assisted by 100–150 ms EC pulse [6]) the absorbed fraction of injected power is ~0.3.

The development of radio frequency wall cleaning as inter-shot conditioning or plasma recovering after disruptions is included in JT-60SA research plan [5]. The gyrotron frequency for this purpose could be either 82 GHz (OM1), 110 GHz (XM2) or 138 GHz (XM2) with short pulse length (~1 s). The conditions for this purpose are very similar to that of EC assisted start-up configuration so useful guidelines could be inferred by dedicated experiments on present devices, as in the case of MST-1 experiments performed on TCV and described in Section 5. In full EC power phase optimal absorption from the plasma is usually high, as confirmed by experiments on present-day machines and beam tracing calculations performed for present and future devices as well like ITER and JT-60SA itself, with plasma optical depth $\tau > 10$ in these scenarios, giving a fraction of absorbed power close to unity (>99%). Lower absorption may occur for far off-axis injection (85% for outer deposition locations with normalized toroidal radius $\rho = 0.9$), with polarization mismatches due to not optimal wave coupling and in the case of high density operations due to the presence of cutoff plasma frequency ($\propto n_e^{1/2}$) refracting the beam along the wave path.

3. Wall loads and diffuse stray radiation detection

As described in Section 2 there are phases of EC operation that may have low or negligible absorption with respect to reference scenarios operations. In these circumstances, the plasma presence is neglected to describe the effect of the injected RF power on the chamber wall and on sensitive equipment. As a first rough assumption, the wall is described as a plane perfect reflector: the

[1] The pair of poloidal and toroidal launching angles (α, β) can be defined and expressed in terms of the cylindrical components of the wave vector as follows: $k_R = \cos\alpha \cos\beta$, $k_\phi = \sin\beta$, $k_z = -\cos\alpha \sin\beta$ to give $\tan\alpha = k_z/k_R$ and $\sin\beta = k_\phi$.

wall structure and the wall shape are not taken into account for simplicity. After some reflections we assume that the radiation inside the tokamak chamber cannot be anymore described as a collimated beam but, on the contrary, can be described as diffuse (stray), depolarized radiation. The breakdown requires up to 1 MW injected from the EC launcher, full EC operations 7 MW. The following results have been obtained considering the injection of a single beam (1 MW) from the focusing mirror of the antenna.

3.1. Direct illumination and stray radiation

The peak intensity at an axial distance z from the beam waist is given by $I(0,z) = 2P_0/(\pi w_x(z)w_y(z))$ [W/m^2] and describes the power density on the axis of the single beam. This represents the peak power at the beam incident location. The average power loading is estimated considering the whole transmitted power distributed over the projection of the beam on the chamber wall at the reflecting points. The beam is considered to have an elliptical cross section with axis $2w_x(z)$ and $2w_y(z)$ (where w_x and w_y are the beam radii on the x and y directions of the astigmatic beam at distance z from the launching mirror). The beam size considered includes in this approximation more than 99.97% of the transmitted power in the fundamental Gaussian mode. Another simplification is to consider flat the wall where the beam is reflected. The average power loading is:

$$P(z) = \frac{P_0}{4\pi(w_x(z)/(\cos(\alpha_i)))w_y(z)} \ [\mathrm{W/m^2}] \quad (1)$$

where α_i is the beam incident angle. With respect to the poloidal plane passing through the center of the launching mirror, different injection directions are considered: 0° in toroidal direction (pure poloidal injection) and four poloidal angles ($\alpha = 20°, \alpha = 0°$ and $\alpha = -40°$), shown in Fig. 1 and listed in Table 1. The angles $\alpha = 20°$ and $\alpha = -40°$ correspond to mechanical antenna limits (the latter giving possible back reflection due to the local geometry of the stabilizing plate), $\alpha = -20°$ could be used in case of assisted breakdown configurations allowing 2 efficient passes into vessel regions where the magnetic field null is expected. $\alpha = 0°$ is a potentially dangerous launch angle due to the normal incidence on inner wall while $\alpha = -35.5°$ may be used at the beginning of JT-60SA operations (orientation of straight waveguide).

As a general feature the power density at the second bounce is about 1/3 the power density at first bounce. Moreover, the worst cases are found for the 1st bounce at 0° (normal incidence) and for the 2nd bounce at 20° (shortest path and thus lower beam diffraction) and at −40° (normal incidence on stabilizing plate). In the environment of the electromagnetic code GRASP©, the path of the central ray of the beam can be simulated with geometrical optics. A section of the first wall and stabilizing plate [5] have been implemented in the model to study multiple reflections and stray-light directions for particular launching configurations, as shown in Fig. 2. Considering a toroidal section of the model, the two shown cases refer to large variations of the poloidal injection angles, both ending in ray directions back into the aperture. The model can be useful to explore the implications of multiple bouncing in critical areas (i.e. divertor area) and quantitative analysis of the wall loads in low absorption scenarios.

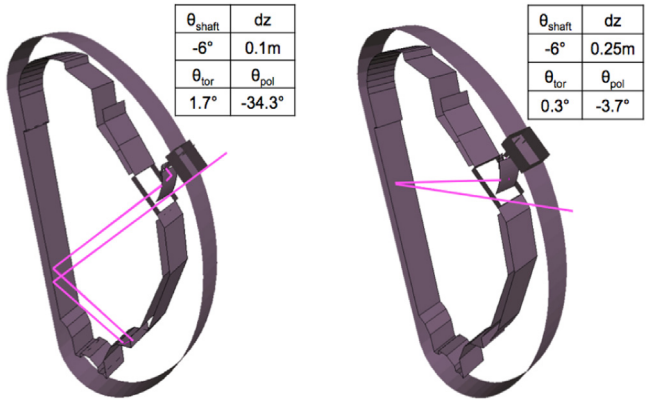

Fig. 2. Two sketches of the GRASP model with a section of the first wall, the stabilizing plate with aperture and the launcher. The pink line represents the central ray path in geometrical optics. For each case the table indicates toroidal and poloidal (θ_{tor} and θ_{pol}) launching angles corresponding to mechanical parameters (θ_{shaft} and dz).

With a simplified model [9], the amount of expected diffuse stray radiation can also be estimated. Following [9] the stray radiation power density is given by:

$$P_s = P_{tot}\frac{1-\alpha_p}{\alpha_W A_W + \langle\alpha_p\rangle A_p + A_a} \ [\mathrm{W/m^2}] \quad (2)$$

where P_{tot} is the EC input power, α_p the single pass absorption coefficient in a given scenario, α_W and A_W the absorption coefficient and area of the wall surface respectively, $\langle\alpha_p\rangle$ and A_p the average absorption of isotropic radiation in the plasma and plasma surface, and A_a the area of the vessel apertures. Typical and reasonable values expected for selected JT-60SA scenarios are summarized in Table 2.

In the limit case corresponding to EC power injection into empty chamber with no absorption at all in the plasma the stray amount would be 28.6 kW/m^2 for 1 MW injected and ∼200 kW/m^2 in the case of full EC power pulse (7 MW).

3.2. Detectors for machine protection

When machine protection becomes a primary driver, safety systems must ensure prompt reaction and detectors using the pyroelectric effect may be suitable to monitor fast the changes of EC stray intensity. In these detectors the output signal is proportional to the temperature variation experienced by the sensible area of

Table 1
Preliminary evaluations of direct irradiation effects were done (1 MW beam, simplified geometry, no plasma absorption, polarization effects not included).

f [GHz]	α [deg]	1st bounce		2nd bounce	
		$I(0,z)$MW/m^2	$P(z)$MW/m^2	$I(0,z)$MW/m^2	$P(z)$MW/m^2
110	20	26.5	3.1	11.0	1.1
	0	28.5	3.6	6.9	0.9
	−20	25.2	3.0	7.2	0.9
	−35.5	19.0	1.9	7.7	0.9
	−40	16.5	1.6	8.3	1.0
138	20	31.5	3.7	13.1	1.3
	0	33.9	4.2	8.3	1.0
	−20	30.0	3.5	8.6	1.1
	−35.5	22.3	2.3	9.2	0.7
	−40	19.7	1.9	10.1	1.3

Table 2
Stray radiation power density evaluation in case of specific scenarios and with JT-60SA vessel characteristics as included in the Plant Design Integration document.

Parameter	Ass. BKD	Ref. Scen.	Empty vessel
Ptot	1	7.0	∼0.15 (blips)
α_p	<0.5	0.99	0
α_W		0.013 [SS] 0.008 [CFC]	
A_W [m^2]		283	
$\langle\alpha_p\rangle$	0.1	0.1	0
A_P [m^2]		52.6	
A_a [m^2]		23.7	
P_s [kW/m^2]	15.3 [SS], 16.0 [CFC]	2.1 [SS], 2.2 [CFC]	4.6 [SS], 4.8 [CFC]

the detector. Despite the pyrodetectors may be suitable to monitor the fast changes in the level of stray radiation, it has to be pointed out that no solution could grant complete elimination of risks. The response speed of a pyroelectric detector usually is limited by its electrical circuit design rather than by its thermal properties. The rise time of the response can in principle extend to the 10^2–10^3 μs regime for mm-wave radiation. The typical aperture size is ∼5 mm^2 with field of view >75° and thermal time constant $\tau_D \sim 150$ ms. With this respect, such an ECH safety system is meant to protect tokamak windows against strong localized EC power deposition and not meant to protect all the systems that are behind the windows.

4. System and layout proposal for JT-60SA

As previously mentioned, experience from present devices [8] indicates that EC stray is toroidally inhomogeneous thus a hybrid layout for different monitoring levels seems to be the most promising solution for JT-60SA. In this proposal, direct illumination and/or reflected beams can be detected by fast pyrodetectors in proximity of EC ports vacuum windows and potentially accessible nearby aperture granting safety operations.

Regarding stray radiation measurements on the other hand, being fast detectors still a good solution, sniffer probes or pick-up waveguides can be beneficial if mounted at specific tokamak locations, providing response typical of multi-modal antenna, with sensitivity approximately constant for any linear polarization, low directivity and designed to collect all incoming mm-wave wave radiation. It has to be pointed out in fact that the signal coming from sniffer probes is normally characterised by large deviations, which can be comparable to the signal amplitude. The plasma itself acts as phase mixer for the stray radiation field, affecting the mode spectrum collected by the probe. For real-time applications of this signal, a low pass filter is mandatory, at the expense of temporal resolution and time response efficiency, together with averaging over time, which for our purposes drives the preference for detectors with faster response like the pyrodetectors. Fig. 3 shows an example of possible mounting when probes design is inserted into JT-60SA model. A minimum number $N = 23$ detectors (19 “fast”, 4 “slow”) has been identified to be proposed and located as follows: 6 detectors for sectors P-01, P-04 (EC and diagnostic ports), 5 located at sector P-08 (EC and diagnostic port), 3 at sector P-11. This set could be installed at a first stage and involving just EC ports locations [5] and at a later one, depending on machine configuration, an additional set of detectors may be mounted: 1 at diagnostic sector P-09 and 4 located at top and bottom of tokamak vessel. 4 sniffer probes (or D-band WG) could then be installed P-06, P-13, P-15 and P-17.

5. System operations during ECRH wall conditioning experiment on TCV

Wall conditioning will be required in JT-60SA to control fuel and impurity recycling and to improve plasma performance and reproducibility. EC Wall Conditioning (ECWC) experiments in helium were performed on TCV using in the framework of EUROfusion MST-1 campaign with a similar ECRH configuration in preparation of JT-60SA operations [10]. Available gyrotrons operating at 82.7 GHz (XM2) were used with nearly perpendicular injection mimicking the configuration envisaged in JT-60SA. Single-path absorption of the EC wave is low in the optically thin ECWC plasmas and TCV stray detectors were used to monitor the amount of non absorbed radiation in the different configurations explored. The safety system available (∼30 pyrodetectors mounted on most of the vacuum windows (an example is shown in Fig. 3 right) provided additional indications for the most favourable operating conditions and thus acted as a useful diagnostic probe of stray radiation.

As an example, the feature of a delayed breakdown in the early phase of the discharge as a function of the experimental parameters was monitored by stray detectors response in TCV discharges 51520, 51523 and 51546 (the time traces of a detectors signal are shown in Fig. 4 left) when XM2 was launched from TCV Sectors7 at 0.2 s. Prompt rise in detectors signals and decrease at breakdown time t_{BKD} due to different absorption conditions was clearly detected by the stray system. Additionally, in the case of the TCV discharge 51960, where a poloidal scan was performed to find optimal injection angle with θ sweeping from 10° to 35.5°, we clearly obtained response from the pyrodetector confirming the favourable injection. This is shown in Fig. 4 right, where the stray signal grows to higher level with θ approaching to larger angles, far form the ideal condition of multiple pass absorption.

Despite similarities with respect to foreseen applications of ECRH like wall conditioning or assisted start up in the two devices, TCV and JT-60SA will differ to a large extent when full power, long

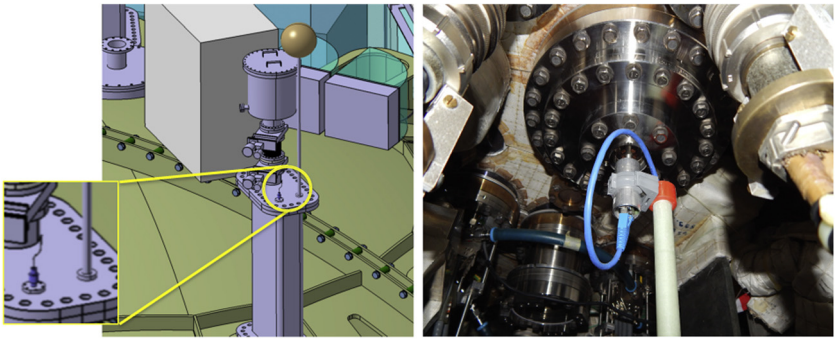

Fig. 3. Left: possible installation of stray radiation detectors on a vertical port of JT-60SA. The pyrodetector, has smaller dimension when compared to the adjacent standard sniffer probe. Right: pyrodetector installed on TCV tokamak (image courtesy of TCV-SPC team).

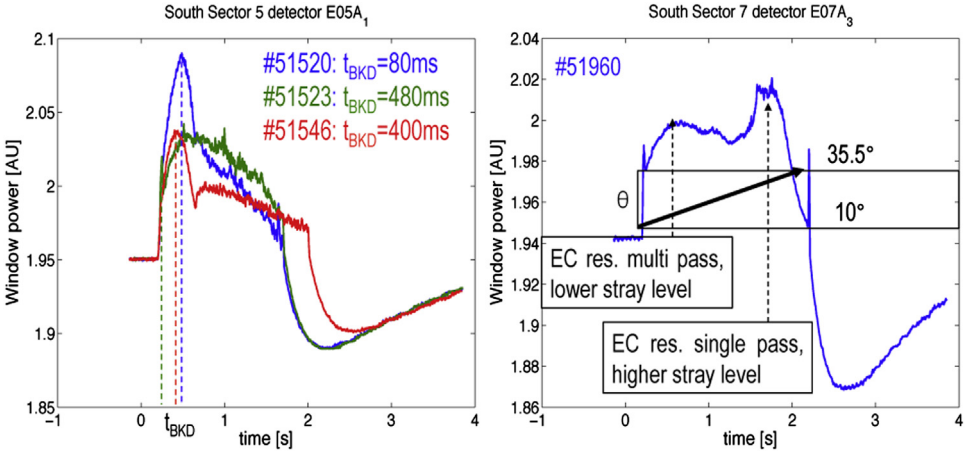

Fig. 4. Data acquired by given detectors during specific ECWC experiments discharges in TCV. Prompt rise in detectors signals and decrease at t_{BKD} well detected by sensors (left). Poloidal scan used to find optimal injection angle with θ (right).

pulse (100 s) and steady state operations are considered. These operations regimes will require more accurate knowledge on the distribution of stray radiation and on the absolute values of the energy flux in the different parts of the machine in order to evaluate how the chosen detectors can be used in an efficient way to prevent damages on machine components from EC stray radiation. In particular, how to ensure long-term stability of the pyrodetector should be better investigated. Possible options could be for example the modulation of the acquired signal or the selective activation and switching off of given sensors during the pulse to compensate signal drifts encountered in the detectors time traces.

6. Conclusions

The general problem of high power radio frequency injection during low absorption operations in tokamaks was here described in the case of JT-60SA. Expected loads and EC stray amount have been qualitatively and quantitatively estimated and the main features of a system capable of prompt detection of high level of EC was here proposed, aiming at machine protection. An example of a similar system now operating on TCV tokamak during EC wall conditioning experiment was also given, with indications and guidelines to provide a conceptual design proposal as a next step. This activity is carried out in the framework of the EUROfusion Consortium and is a part of the WPSA work package and the authors gratefully acknowledge members of the JT-60SA Integrated Project Team for data exchange and fruitful discussions.

Acknowledgements

This work has been carried out within the framework of the EUROfusion Consortium and has received funding from the Euratom Research and Training Programme 2014–2018 under grant agreement No 633053. The views and opinions expressed herein do not necessarily reflect those of the European Commission.

References

[1] Y. Kamada, et al., Nucl. Fusion 53 (2013) 104010.
[2] S. Moriyama, et al., Fusion Eng. Des. 88 (2013) 935–939.
[3] T. Kobayashi, et al., EPJ Web of Conferences, 2015, pp. 04008.
[4] T. Kobayashi, et al., Fusion Eng. Des. 84 (2009) 1063–1067.
[5] JT-60SA Research Unit, http://www.jt60sa.org/pdfs/JT-60SA_Res_Plan.pdf.
[6] G. Granucci, et al., Nucl. Fusion 55 (2005) 093025.
[7] D. Farina, Fusion Sci. Technol. 52 (2007) 154.
[8] M. Schubert, et al., EPJ Web of Conferences, 2015, pp. 02010.
[9] H.J. Hartfuss, et al., Proc. 30th EPS Conf. on Contr. Fusion and Plasma Phys., St. Petersburg, 2003, 27A, O-3.2C.
[10] D. Douai, et al., 26th IAEA Fusion Energy Conf. (Kyoto, Japan), Nucl. Fusion (2016) 8–31.